


RESEARCH ARTICLE

Open Access



# Development and validation of a point-based scoring system for predicting axillary lymph node metastasis and disease outcome in breast cancer using clinicopathological and multiparametric MRI features

Xiaofeng Chen<sup>1,2†</sup>, Zhiqi Yang<sup>1,2†</sup>, Ruibin Huang<sup>3†</sup>, Yue Li<sup>1</sup>, Yuting Liao<sup>4</sup>, Guijin Li<sup>5</sup>, Mengzhu Wang<sup>6</sup>, Xiangguang Chen<sup>1,2</sup>, Zhuozhi Dai<sup>7,8\*</sup>  and Weixiong Fan<sup>1\*</sup>

## Abstract

**Background** Axillary lymph node (ALN) metastasis is used to select treatment strategies and define the prognosis in breast cancer (BC) patients and is typically assessed using an invasive procedure. Noninvasive, simple, and reliable tools to accurately predict ALN status are desirable. We aimed to develop and validate a point-based scoring system (PSS) for stratifying the ALN metastasis risk of BC based on clinicopathological and quantitative MRI features and to explore its prognostic significance.

**Methods** A total of 219 BC patients were evaluated. The clinicopathological and quantitative MRI features of the tumors were collected. A multivariate logistic regression analysis was used to create the PSS. The performance of the models was evaluated using receiver operating characteristic curves, and the area under the curve (AUC) of the models was calculated. Kaplan–Meier curves were used to analyze the survival outcomes.

**Results** Clinical features, including the American Joint Committee on Cancer (AJCC) stage, T stage, human epidermal growth factor receptor-2, estrogen receptor, and quantitative MRI features, including maximum tumor diameter,  $K_{ep}$ ,  $V_e$ , and TTP, were identified as risk factors for ALN metastasis and were assigned scores for the PSS. The PSS achieved an AUC of 0.799 in the primary cohort and 0.713 in the validation cohort. The recurrence-free survival (RFS) and overall survival (OS) of the high-risk ( $> 19.5$  points) groups were significantly shorter than those of the low-risk ( $\leq 19.5$  points) groups in the PSS.

<sup>†</sup>Xiaofeng Chen, Zhiqi Yang and Ruibin Huang contributed equally to the article.

\*Correspondence:

Zhuozhi Dai  
zzdai@stu.edu.cn  
Weixiong Fan  
mrifwx@163.com

Full list of author information is available at the end of the article



© The Author(s) 2023. **Open Access** This article is licensed under a Creative Commons Attribution 4.0 International License, which permits use, sharing, adaptation, distribution and reproduction in any medium or format, as long as you give appropriate credit to the original author(s) and the source, provide a link to the Creative Commons licence, and indicate if changes were made. The images or other third party material in this article are included in the article's Creative Commons licence, unless indicated otherwise in a credit line to the material. If material is not included in the article's Creative Commons licence and your intended use is not permitted by statutory regulation or exceeds the permitted use, you will need to obtain permission directly from the copyright holder. To view a copy of this licence, visit <http://creativecommons.org/licenses/by/4.0/>. The Creative Commons Public Domain Dedication waiver (<http://creativecommons.org/publicdomain/zero/1.0/>) applies to the data made available in this article, unless otherwise stated in a credit line to the data.

**Conclusion** PSS could predict the ALN metastasis risk of BC. A PSS greater than 19.5 was demonstrated to be a predictor of short RFS and OS.

**Keywords** Lymphatic metastasis, Prognosis, Breast neoplasms, Multiparametric magnetic resonance imaging, Risk factors

## Background

Breast cancer (BC) is the most commonly diagnosed cancer among women worldwide and has become the second leading cause of cancer-related death [1]. BC can spread to the regional lymph nodes, primarily to the axillary and internal mammary nodes and subsequently to the medial supraclavicular nodes [2]. Patients with BC frequently experience axillary lymph node (ALN) metastasis, which affects the clinical stage, therapy options, surgical approach, and patient prognosis [1, 2]. Thus, accurate identification of ALN involvement in BC patients is crucial for prognosis and treatment decisions, particularly in the current time of downgrading off axillary surgery. Currently, ALN dissection, sentinel lymph node biopsy (SLNB), and lymph node biopsy before surgery are important procedures for ALN staging. Generally, lymph node biopsy is very important in daily clinical practice for pretreatment staging in patients with suspicious lymph node metastasis. SLNB is the current best standard approach for axillary staging in patients with clinically node-negative BC [3, 4]. ALN dissection is the standard treatment for BC patients with clinically positive nodes, but it might be avoided in patients with negative SLNB, as well as in patients with one or two sentinel lymph node-positivity receiving breast radiation and systemic therapy [5, 6]. However, these are invasive methods with the risk of postoperative complications, especially for ALN dissection [7, 8].

As noninvasive approaches, physical examination, mammography, ultrasonography, and positron emission tomography-computed tomography (PET/CT) are widely used to predict ALN metastasis. However, their abilities to assess the risk of ALN metastasis are limited because of their high false-negative rates and low sensitivity [9–12]. To date, only a few studies have used preoperative MRI to predict ALN metastasis, and these studies have shown that MRI morphological features and enhancement parameters of tumors are correlated with ALN status [13–15]. However, these models have not been widely used due to their complexity in clinical application. Furthermore, the mere identification of ALN metastasis by imaging is insufficient to change the paradigm for axillary surgical strategy [3]. A recently developed and validated nomogram was used to predict the metastasis status of ALNs based on a combination of clinicopathologic and MRI features, in which the

developed model performed well for identifying ALN metastasis [10]. However, using the nomogram might be time-consuming and hard to interpret [16]. Therefore, to simplify the eventual clinical application of the predictive model, a point-based scoring system (PSS) was proposed and has been used to predict lymphovascular invasion and differential diagnosis of tumors [16, 17]. In this study, we aimed to use the PSS to predict the risk of ALN metastasis based on clinicopathological and quantitative MRI features and investigated the prognostic effect of the PSS.

## Materials and methods

### Patient characteristics

This retrospective study was approved by the ethics committee of Meizhou People's Hospital and the requirement for written informed consent was waived. We reviewed a total of 457 consecutive female patients with a postoperative histopathological diagnosis of BC who had undergone preoperative dynamic contrast-enhanced MRI (DCE-MRI) and diffusion-weighted imaging (DWI) scans and axillary biopsy or SLNB (complete ALN dissection was performed if the SLNB or axillary biopsy was positive) from January 2016 to May 2019. The patient exclusion criteria were as follows: (1) patients who had received neoadjuvant therapy prior to breast MRI or surgery; (2) patients with breast cancer recurrence; (3) patients with occult breast cancer; (4) patients with a tumor smaller than 1.0 cm; (5) patients with incomplete clinicopathological data; and (6) patients with poor visualization of the tumors on breast MRI. The patient inclusion/exclusion criteria are shown in Fig. 1. Finally, a total of 219 patients were enrolled and randomly divided into a primary cohort and a validation cohort at a ratio of 7:3 according to previous studies [18, 19]. Histological results after surgery were used as the ground truth of ALN metastasis. This study's patients are part of a large retrospective breast MRI database, of which 165 patients have been reported in a previously published study [20]. A previous report evaluated BC receptor status and molecular subtypes; however, this novel study focused on ALN metastasis by developing a new PSS.

### Clinicopathological characteristics

Clinicopathological data, including age, Ki-67 level, human epidermal growth factor receptor-2 (HER-2),

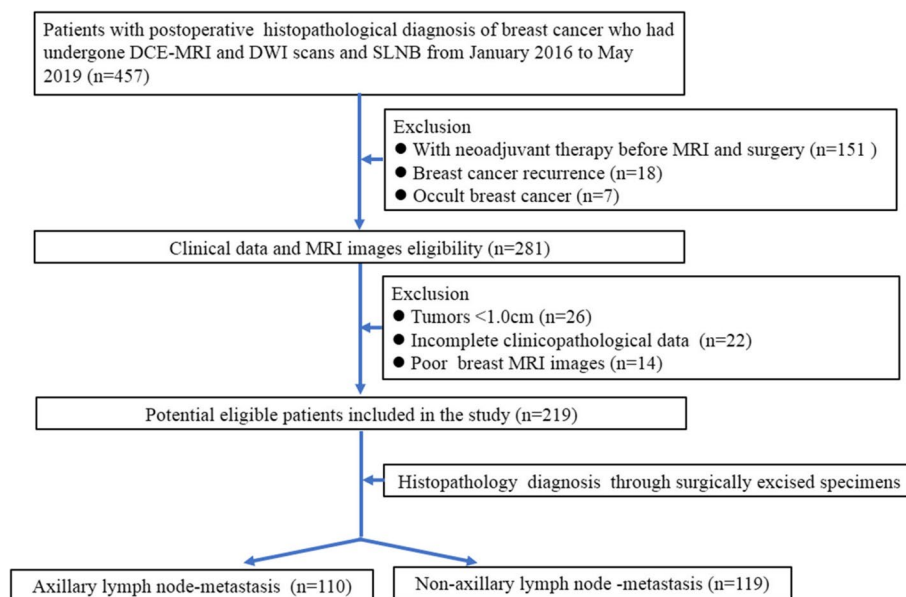


**Fig. 1** Patient selection flowchart

progesterone receptor (PR), estrogen receptor (ER), tumor node metastasis (TNM) stage, American Joint Committee on Cancer (AJCC) stage [21], pathological status of ALNs, number of metastatic ALNs, LVI, and perineural invasion status, were obtained from the patients' medical records. A pathological positive status of ALN metastasis was defined as macrometastasis (foci >2.0 mm) or micrometastasis (foci 0.2–2.0 mm) identified by hematoxylin–eosin staining [7]. LVI was defined as the presence of tumor cells within the space of the endothelial cells [22]. The cutoff value for the positivity of HER-2, PR, and ER was used from internationally recognized standards [23, 24].

### MRI technique

All images were acquired by a 3 T MR system (Magnetom Skyra, Siemens Healthcare) using a 16-channel bilateral breast coil. Table E1 in the supplementary material summarizes the MRI acquisition parameters. The contrast agent gadopentetate dimeglumine (Bayer Pharmaceuticals Corporation) at a dose of 0.2 ml/kg was given by intravenous injection at a rate of 3.0 ml/s.

### Image analysis

MR image analyses were performed on the DCE software package (Tissue 4D, version: syngo MR D13, Siemens Healthcare), and DCE-derived parametric maps were automatically generated after motion correction. Breast tumors were identified on the DCE-MRI images, as the prominent enhancement area corresponded to the high signal area in the DWI image ( $b=800$  s/mm<sup>2</sup>) with

a low signal area on the ADC map. Two radiologists (W.F. and F.C., with more than 15 years of experience) who were both blinded to the clinicopathological data reviewed the DCE-MRI images and ADC maps independently to extract the quantitative parameters of the tumors, including the volume transfer constant ( $K^{\text{trans}}$ , min<sup>-1</sup>), reverse reflux rate constant ( $K_{\text{ep}}$ , min<sup>-1</sup>), extracellular extravascular volume fraction ( $V_e$ ), rate of contrast enhancement for inflow (W-in, min<sup>-1</sup>), rate of contrast decay for outflow (W-out, min<sup>-1</sup>), time to peak enhancement after injection (TTP, min), and ADC value ( $\times 10^{-3}$  mm<sup>2</sup>/s). The region of interest (ROI) drawing principles were as follows (Figure E1 in the supplementary material): ROIs with a minimum area of 0.10 cm<sup>2</sup> were manually drawn on the continuous three maximum sections with the greatest enhancement areas of the tumors, avoiding visible blood vessels, obvious bleeding, and necrotic and cystic areas, with the same position and size on both the DCE-derived parametric maps and the ADC maps. The mean values of the parameters were taken as the final values. In addition, tumor sizes, including the maximum, minimum, and effective diameter of the tumor on the largest section, were recorded on the DCE-MRI images.

### Clinical treatment

All patients underwent surgical treatment after breast MRI. The surgical methods for BC include breast-conserving surgery, mastectomy, and breast reconstruction surgery, which were determined by the National Guidelines for the Diagnosis and Treatment of

Breast Cancer 2022 in China (English version)[23]. Of 219 patients, 21 patients had received breast-conserving surgery, 189 patients had received mastectomy, and 9 patients had received breast reconstruction surgery. Furthermore, 171 patients received adjuvant chemotherapy after surgery, 71 received radiation therapy after surgery, and 121 received adjuvant endocrine therapy after surgery. Moreover, 43 patients had received all three treatment methods after surgery.

#### Follow-up

All patients underwent clinical and imaging follow-up with chest CT, breast mammography, or breast MRI until progression, followed by routine follow-up until death. According to the Chinese Anti-Cancer Association guidelines for the diagnosis and treatment of breast cancer (2021 version), all patients were postoperatively followed up with a physical examination, laboratory tests, CT, mammography, and ultrasound every 3 months for the first two years, once every 6 months during years 3 to 5, and once a year after 5 years. Additionally, the patients with breast-conserving surgery were followed up with breast MRI once a year. Recurrence-free survival (RFS) was measured in months from the date of surgery to the first date of local recurrence, distant metastasis, or the last follow-up date, whichever came first. Overall survival (OS) was measured in months from the date of surgery to the date of death or the last follow-up date. The last follow-up date was March 1, 2021.

#### Point-based scoring system development

A PSS was constructed using the method described by Sullivan et al. [25]. Continuous variables were transformed into binary variables according to the cutoff values determined by the largest Youden index to reduce the PSS score range and simplify its eventual clinical application. In the primary cohort, the cutoff values for age, maximum tumor diameter, minimum tumor diameter, effective tumor diameter,  $K^{trans}$ ,  $K_{ep}$ ,  $V_e$ , W-in, W-out, TTP, and ADC were 48.5 years, 3.55 cm, 1.95 cm, 3.13 cm,  $0.298 \text{ min}^{-1}$ ,  $0.982 \text{ min}^{-1}$ , 0.253,  $0.674 \text{ min}^{-1}$ ,  $-0.013 \text{ min}^{-1}$ , 0.778 min, and  $0.736 \times 10^{-3} \text{ mm}^2/\text{s}$ , respectively. All variables were included in the multivariate logistic regression analysis following the backward stepwise selection method. The point of each selected variable was assigned based on its  $\beta$ -coefficient in the multivariate logistic regression analysis and rounded to the nearest 0.5. The final PSS score was obtained by summing the points of each variable. The odds ratios (ORs) with 95% confidence intervals (CIs) of each variable were also calculated.

#### Statistical analysis

R version 3.6.0 was used for statistical analysis. Continuous variables with a normal distribution are expressed as the mean  $\pm$  standard deviation, and categorical variables are expressed as counts and percentages. Data between the ALN metastasis and non-ALN metastasis groups were compared with Student's t test, chi-squared test, or Kruskal–Wallis H test, if appropriate. In addition, the intraclass correlation coefficient (ICC) was used to assess the interobserver agreement of the DCE-MRI parameters and the ADC values between the two radiologists [26, 27]. An ICC value between 0.61 and 0.80 indicates good agreement, while an ICC value  $\geq 0.81$  indicates excellent agreement [28]. A receiver operating characteristic (ROC) curve was created to estimate the discriminating power of the models, and the area under the curve (AUC), accuracy, sensitivity and specificity were calculated [27]. The ROCs of the models were compared by using the DeLong test. For the survival analysis, the patients were divided into low-risk and high-risk groups according to the PSS point, and the grouping threshold was determined by the X-tile method [29]. Kaplan–Meier curves for the high-risk and low-risk groups were plotted, and the prognosis of the high- and low-risk groups was compared by using the log rank test.  $P < 0.05$  was considered statistically significant.

## Results

#### Patient characteristics

Of 219 patients, 110 patients had non-ALN metastasis and 109 patients had ALN metastasis. The characteristics of the patients in the total, primary, and validation cohorts are listed in Table 1. The ALN metastasis positivity was 49.7% (76/153) and 50.0% (33/66) in the primary cohort and validation cohort, respectively. The patients with ALN metastasis had higher maximum, minimum, and effective tumor diameters, and higher T stages than the patients without ALN metastasis in the total, primary, and validation cohorts (all  $P < 0.05$ ). Compared to the patients without ALN metastasis, higher positive rates of LVI and lower  $V_e$  and W-out values were more pronounced in the patients with ALN metastasis in the total and primary cohorts (all  $P < 0.05$ ), but these differences were not confirmed in the validation cohort (all  $P > 0.05$ ). In addition, the patients with ALN metastasis had a higher Ki-67 index than patients without ALN metastasis in the total cohort ( $P = 0.038$ ), but this was not confirmed in the primary and validation cohorts (all  $P > 0.05$ ).

**Table 1** Characteristics of patients with and without axillary lymph node metastasis

Characteristics	Total cohort (n = 219)			Primary cohort (n = 153)			Validation cohort (n = 66)		
	Non-ALN metastasis (n = 110)	ALN metastasis (n = 109)	P	Non-ALN metastasis (n = 77)	ALN metastasis (n = 76)	P	Non-ALN metastasis (n = 33)	ALN metastasis (n = 33)	P
Age (years)	51.85 ± 10.68	49.91 ± 11.13	0.191 <sup>a</sup>	52.04 ± 10.71	51.13 ± 11.87	0.620 <sup>a</sup>	51.39 ± 10.78	47.10 ± 8.74	0.080 <sup>a</sup>
Maximum diameter (cm)	2.74 ± 1.03	3.63 ± 1.59	<b>&lt; 0.001<sup>a</sup></b>	2.73 ± 1.04	3.53 ± 1.54	<b>&lt; 0.001<sup>a</sup></b>	2.78 ± 1.01	3.87 ± 1.70	<b>0.003<sup>a</sup></b>
Minimum diameter (cm)	1.80 ± 0.63	2.30 ± 1.02	<b>&lt; 0.001<sup>a</sup></b>	1.80 ± 0.63	2.28 ± 1.05	<b>0.001<sup>a</sup></b>	1.81 ± 0.65	2.33 ± 0.99	<b>0.014<sup>a</sup></b>
Effective diameter (cm)	2.27 ± 0.78	2.97 ± 1.22	<b>&lt; 0.001<sup>a</sup></b>	2.26 ± 0.79	2.91 ± 1.20	<b>&lt; 0.001<sup>a</sup></b>	2.30 ± 0.77	3.10 ± 1.27	<b>0.003<sup>a</sup></b>
Perineural invasion			0.542 <sup>b</sup>			0.479 <sup>b</sup>			1.000 <sup>b</sup>
Negative	105(95.45%)	102(93.58%)		74(96.10%)	70(92.11%)		31(93.94%)	32(96.97%)	
Positive	5(4.55%)	7(6.42%)		3(3.90%)	6(7.89%)		2(6.06%)	1(3.03%)	
LVI			<b>0.014<sup>b</sup></b>			<b>0.034<sup>b</sup></b>			0.202 <sup>b</sup>
Negative	93(84.55%)	77(70.64%)		64(83.12%)	52(68.42%)		29(87.88%)	25(75.76%)	
Positive	17(15.45%)	32(29.36%)		13(16.88%)	24(31.58%)		4(12.12%)	8(24.24%)	
ER			0.959 <sup>b</sup>			0.542 <sup>b</sup>			0.306 <sup>b</sup>
Negative	40(36.36%)	40(36.70%)		30(38.96%)	26(34.21%)		10(30.30%)	14(42.42%)	
Positive	70(63.64%)	69(63.30%)		47(61.04%)	50(65.79%)		23(69.70%)	19(57.58%)	
PR			0.453 <sup>b</sup>			0.939 <sup>b</sup>			0.138 <sup>b</sup>
Negative	56(50.91%)	61(55.96%)		41(53.25%)	40(52.63%)		15(45.45%)	21(63.64%)	
Positive	54(49.09%)	48(44.04%)		36(46.75%)	36(47.37%)		18(54.55%)	12(36.36%)	
HER-2			0.848 <sup>b</sup>			0.764 <sup>b</sup>			0.438 <sup>b</sup>
Negative	76(69.09%)	74(67.89%)		53(68.83%)	54(71.05%)		23(69.70%)	20(60.61%)	
Positive	34(30.91%)	35(32.11%)		24(31.17%)	22(28.95%)		10(30.30%)	13(39.39%)	
Ki-67			<b>0.038<sup>b</sup></b>			0.117 <sup>b</sup>			0.159 <sup>b</sup>
< 20%	37(33.64%)	23(21.10%)		26(33.77%)	17(22.37%)		11(33.33%)	6(18.18%)	
≥ 20%	73(66.36%)	86(78.90%)		51(66.23%)	59(77.63%)		22(66.67%)	27(81.82%)	
T stage			<b>&lt; 0.001<sup>c</sup></b>			<b>&lt; 0.001<sup>c</sup></b>			<b>0.028<sup>c</sup></b>
T1	49(44.55%)	21(19.27%)		35(45.45%)	14(18.42%)		14(42.42%)	7(21.21%)	
T2	58(52.73%)	70(64.22%)		41(53.25%)	51(67.11%)		17(51.52%)	19(57.58%)	
T3	1(0.91%)	11(10.09%)		0(0.00%)	5(6.58%)		1(3.03%)	6(18.18%)	
T4	2(1.82%)	7(6.42%)		1(1.30%)	6(7.89%)		1(3.03%)	1(3.03%)	
M stage			0.671 <sup>b</sup>			0.239 <sup>b</sup>			1.000 <sup>b</sup>
M0	108(98.18%)	105(96.33%)		77(100.00%)	73(96.05%)		31(93.94%)	32(96.97%)	
M1	2(1.82%)	4(3.67%)		0(0.00%)	3(3.95%)		2(6.06%)	1(3.03%)	
AJCC stage			0.241 <sup>c</sup>			0.615 <sup>c</sup>			0.165 <sup>c</sup>
I	22(20.00%)	12(11.01%)		15(19.48%)	10(13.16%)		7(21.21%)	2(6.06%)	
II	46(41.82%)	47(43.12%)		32(41.56%)	33(43.42%)		14(42.42%)	14(42.42%)	
III	18(16.36%)	30(27.52%)		12(15.58%)	19(25.00%)		6(18.18%)	11(33.33%)	
IV	24(21.82%)	20(18.35%)		18(23.38%)	14(18.42%)		6(18.18%)	6(18.18%)	
MRI parameters									
K <sup>trans</sup> (min <sup>-1</sup> )	0.22 ± 0.12	0.19 ± 0.12	0.058 <sup>a</sup>	0.22 ± 0.11	0.19 ± 0.11	<b>0.047<sup>a</sup></b>	0.21 ± 0.14	0.20 ± 0.14	0.598 <sup>a</sup>
K <sub>ep</sub> (min <sup>-1</sup> )	0.82 ± 0.25	0.86 ± 0.22	0.269 <sup>a</sup>	0.84 ± 0.24	0.85 ± 0.23	0.756 <sup>a</sup>	0.79 ± 0.29	0.88 ± 0.20	0.144 <sup>a</sup>
V <sub>e</sub>	0.27 ± 0.13	0.22 ± 0.12	<b>0.006<sup>a</sup></b>	0.27 ± 0.12	0.22 ± 0.11	<b>0.022<sup>a</sup></b>	0.29 ± 0.15	0.23 ± 0.15	0.115 <sup>a</sup>
W-in (min <sup>-1</sup> )	0.57 ± 0.21	0.60 ± 0.27	0.368 <sup>a</sup>	0.56 ± 0.19	0.59 ± 0.27	0.365 <sup>a</sup>	0.59 ± 0.26	0.61 ± 0.28	0.775 <sup>a</sup>
W-out (min <sup>-1</sup> )	-0.01 ± 0.02	-0.02 ± 0.02	<b>0.002<sup>a</sup></b>	-0.01 ± 0.02	-0.02 ± 0.02	<b>0.009<sup>a</sup></b>	-0.01 ± 0.02	-0.02 ± 0.02	0.081 <sup>a</sup>
TTP (min)	0.67 ± 0.19	0.67 ± 0.20	0.983 <sup>a</sup>	0.67 ± 0.19	0.68 ± 0.20	0.803 <sup>a</sup>	0.67 ± 0.21	0.65 ± 0.21	0.698 <sup>a</sup>
ADC (× 10 <sup>-3</sup> mm <sup>2</sup> /s)	0.87 ± 0.15	0.84 ± 0.13	0.158 <sup>a</sup>	0.87 ± 0.14	0.84 ± 0.15	0.239 <sup>a</sup>	0.86 ± 0.17	0.83 ± 0.09	0.447 <sup>a</sup>

Notes. P<sup>a</sup>: Student's t test, P<sup>b</sup>: chi-squared test, P<sup>c</sup>: Kruskal–Wallis H test

Abbreviations: ALN Axillary lymph node, LVI Lymphovascular invasion, ER Estrogen receptor, PR Progesterone receptor, HER-2 Human epidermal growth factor receptor-2, ADC Apparent diffusion coefficient



**Table 2** Multivariate logistic regression analysis for predicting axillary lymph node metastasis with the assigned points

Variables	Multivariate regression			
	Odds Ratio (95% CI)	P value	$\beta$ -Coefficient	Points
AJCC stage				
I	reference	-	-	0
II	2.28 (0.75~7.27)	0.151	0.825	1.0
III	37,836,559.51 (0~NA)	0.988	17.448	17.5
IV	9,984,898.98 (0~NA)	0.989	16.116	16.0
T stage				
T1	reference	-	-	0
T2	3.11 (1.3~8)	0.014	1.359	1.0
T3	27,337,664.44 (0~NA)	0.990	17.123	17.0
T4	8.59 (0.83~205.36)	0.097	2.150	2.0
ER				
Negative	reference	-	-	0
Positive	10,968,914.8 (0~NA)	0.989	16.21	16.0
HER-2				
Negative	reference	-	-	0
Positive	0.25 (0.07~0.84)	0.310	-1.388	-1.5
Maximum tumor diameter category (cm)				
< 3.55	reference	-	-	0
$\geq 3.55$	3.17 (1.26~8.45)	0.017	1.154	1.0
$K_{ep}$ category ( $\text{min}^{-1}$ )				
< 0.982	reference	-	-	0
$\geq 0.982$	2.50 (0.98~6.66)	0.059	0.918	1.0
$V_e$ category				
< 0.253	reference	-	-	0
$\geq 0.253$	0.52 (0.24~1.13)	0.101	-0.652	-0.5
TTP category (min)				
< 0.778	reference	-	-	0
$\geq 0.778$	3.23 (1.27~8.74)	0.017	1.176	1.0

Abbreviations: CI Confidence intervals, ER Estrogen receptor, PR Progesterone receptor

### Agreement between two readers

The ICC values between the two readers for  $K^{trans}$ ,  $K_{ep}$ ,  $V_e$ , W-in, W-out, TTP, and ADC were 0.995 (95% CI: 0.994–0.996), 0.775 (95% CI: 0.716–0.823), 0.988 (95% CI: 0.984–0.990), 0.990 (95% CI: 0.988–0.993), 0.793 (95% CI: 0.739–0.838), 0.965 (95% CI: 0.955–0.973), and 0.894 (95% CI: 0.863–0.917), respectively.

### Point-based scoring system development based on the primary cohort

Based on the backward stepwise selection method in the multivariate logistic regression analysis (Table 2), eight variables were associated with ALN metastasis and they were assigned scores for the final prediction rule: AJCC stage [II (1.0 points), III (17.5 points), IV (16.0 points)], T stage [T2 (1.0 points), T3 (17.0 points), T4 (2.0 points)], ER (positive, 16.0 points), HER-2 (positive, 1.5 points), maximum tumor diameter ( $\geq 3.55$  cm, 1.0 points),  $K_{ep}$  ( $\geq 0.982 \text{ min}^{-1}$ , 1.0 points),  $V_e$  ( $\geq 0.253$ , -0.5 points), and TTP ( $\geq 0.778 \text{ min}^{-1}$ , 1.0 points). The PSS point threshold for predicting the risk of ALN metastasis was 17.5, as obtained by the largest Youden index.

### Performance of the point-based scoring system

The logistic regression model that used all of the predictors for ALN metastasis obtained an AUC of 0.802 in the primary cohort and 0.707 in the validation cohort, and the PSS achieved an AUC of 0.799 in the primary cohort and 0.713 in the validation cohort (Table 3). ROC curve comparisons between the logistic regression model and the PSS are shown in Fig. 2. There were no significant AUC differences between the logistic regression model and PSS in either the primary cohort ( $P=0.645$ ) or in the validation cohort ( $P=0.572$ ). Table 4 presents the risk of ALN metastasis according to the PSS, and the ALN metastasis risk ranged from 4.7% to 100.0%. Figure 3 and Fig. 4 represent examples of the PSS in use.

### Predictors of survival

All patients had completed RFS follow-up, and the median RFS of all patients was 32 [interquartile range (IQR): 23.0–44.0] months, of which 26 patients had tumor recurrence and 193 patients had no tumor recurrence. The recurrence rate was 19.3% in the ALN metastasis group and 4.5% in the non-ALN metastasis group. In addition, 9 patients with tumor recurrence were deceased and 2 patients without tumor recurrence were deceased. While 218 patients had completed OS follow-up, the median OS of all patients was 43.8 (IQR: 32.0–55.0) months, of which 11 patients were

**Table 3** Performance of the prediction model for axillary lymph node metastasis

	Primary cohort				Validation cohort			
	AUC(95% CI)	Accuracy	Sensitivity	Specificity	AUC(95% CI)	Accuracy	Sensitivity	Specificity
Logistic regression model	0.802(0.733–0.871)	0.732	0.816	0.649	0.707(0.576–0.838)	0.712	0.697	0.727
PSS	0.799(0.731–0.868)	0.725	0.776	0.675	0.713(0.585–0.840)	0.697	0.667	0.727

Abbreviations: PSS Point-based scoring system, CI Confidence intervals

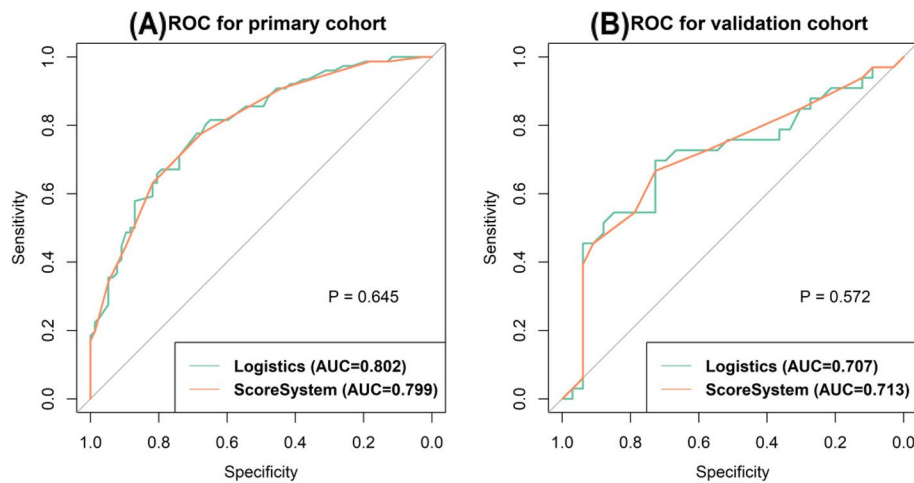


**Fig. 2** Receiver operator characteristic (ROC) curve for the prediction models in the primary cohort (A) and validation cohort (B)

**Table 4** Axillary lymph node metastasis risk according to the point-based scoring system

Risk score	ALN metastasis risk	Total number	Number of ALN metastasis
15	4.7%	4	1
15.5	7.6%	11	1
16	11.9%	6	1
16.5	18.2%	35	9
17	26.9%	41	14
17.5	37.8%	29	13
18	50.0%	26	18
18.5	62.2%	19	11
19	73.1%	17	13
19.5	81.8%	5	4
20	88.1%	3	3
20.5	92.4%	3	3
31	100%	1	1
33	100%	1	1
33.5	100%	2	2
34	100%	4	4
34.5	100%	1	1
35	100%	3	3
35.5	100%	3	2
36	100%	1	1
49.5	100%	1	1
50	100%	2	1
52.5	100%	1	1
Total	49.8%	219	109

Note. ALN Axillary lymph node

deceased. Of note, the overall death rate was 8.3% in the ALN metastasis group and 1.8% in the non-ALN metastasis group.

The PSS point threshold for the low-risk group and high-risk group was 19.5, as obtained by the X-tile method [29]. The median RFS was 32.0 (IQR:15.5–46.0) months for the high-risk group (>19.5 points) and 32.5 (IQR:22.9–44.3) for the low-risk group (≤19.5 points) in the primary cohort (the comparative *P* value for the two survival curves using the log-rank test was lower than 0.0001, hereinafter, Fig. 5A) and 32.0 (IQR:21.0–40.0) months for the high-risk group and 32.0 (IQR:23.5–40.0) for the low-risk group in the validation cohort (*P*=0.032, Fig. 5B). The Kaplan–Meier survival analysis showed that the median OS was 43.3 (IQR:31.9–56.0) months for the high-risk group and 50.0 (IQR:29.0–55.5) for the low-risk group in the primary cohort (*P*=0.042, Fig. 6A) and 43.5 (IQR:32.0–55.0) months for the high-risk group and 50.5 (IQR:45.0–55.0) for the low-risk group in the validation cohort (*P*=0.029, Fig. 6B).

### Discussion

In the present study, we developed and validated a PSS for stratifying the ALN metastasis risk of BC based on the combination of clinical features and quantitative MRI features and investigated the prognostic effect of the PSS. Our results showed that the PSS has good discrimination for stratifying the ALN metastasis risk of BC in the primary cohort and in the validation cohort. In addition, the RFS and OS of the high-risk group (>19.5 points) patients were significantly lower than those of the low-risk (≤19.5 points) group patients in the PSS.

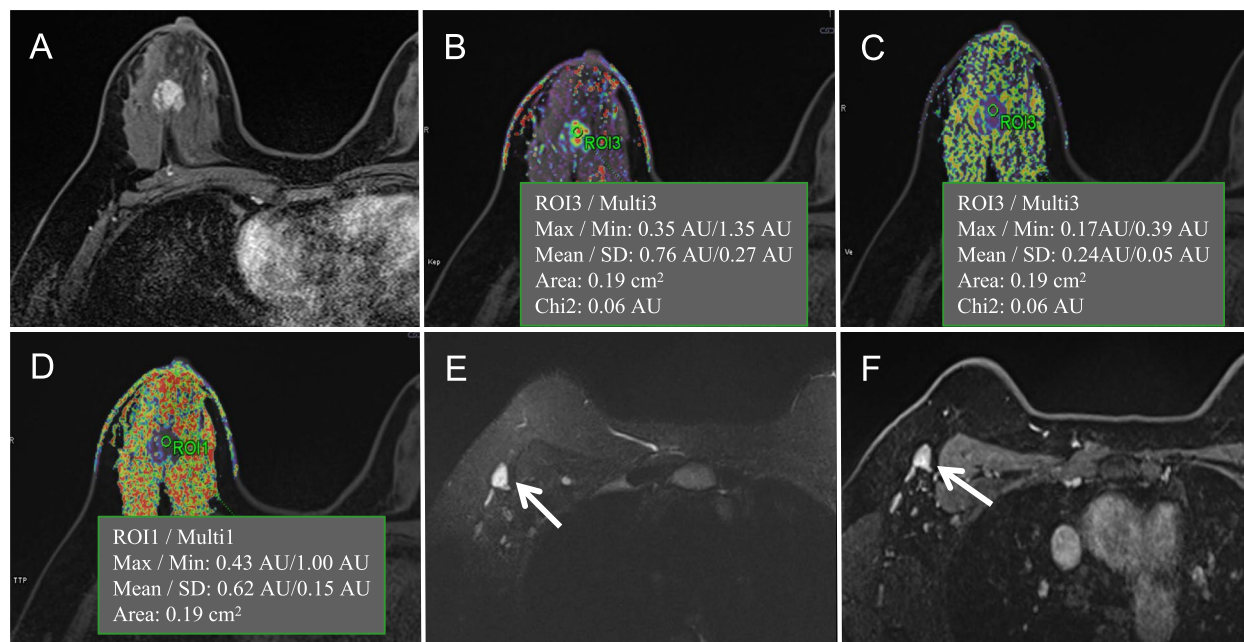


**Fig. 3** One example of the point-based scoring system for predicting breast cancer patients without axillary lymph node metastasis. **A–F** are MRI images of a female right breast cancer patient with invasive ductal carcinoma who was positive for human epidermal growth factor receptor-2, negative for estrogen receptor, AJCC stage III, and T2 stage. An axial contrast-enhanced  $T_1$ WI image (**A**) shows a tumor with a maximum diameter of 2.3 cm located in the lower-outer quadrant. The mean values of  $K_{ep}$ ,  $V_e$  and TTP from the corresponding pseudocolor images of  $K_{ep}$  (**B**),  $V_e$  (**C**), and TTP (**D**) were 0.760 min<sup>-1</sup>, 0.190, and 0.620 min, respectively. Breast MRI was suspicious for axillary lymph node metastasis based on the following features: axial  $T_2$ WI with fat suppression imaging (**E**) and axial contrast-enhanced  $T_1$ WI imaging (**F**) showing cortical thickening, an oval shape and a long-to-short axis ratio of 1.4 for a maximal lymph node (white arrow) in axillary level I (nodes lateral and inferior to pectoralis minor muscle). However, the risk of axillary lymph node metastasis assessed by the scoring system was 17.0, with an axillary lymph node metastasis probability of 26.9%. The final postoperative pathology report showed that this tumor had no axillary lymph node metastasis

Risk stratification scoring systems have been used to guide clinical decision-making [16, 30–33]. A recent study conducted by MY et al. developed a scoring system to stratify the risk of lymphovascular invasion in BC patients with an AUC of 0.824 [16]. Another study from Ouldame et al. used a scoring system to predict axillary response after neoadjuvant chemotherapy in initially node-positive women with BC [34]. However, little is known about the ALN based on this scoring system. In this study, to develop the risk stratification scoring system, a multivariable logistic regression analysis was used to select the risk factors for ALN metastasis. The PSS point threshold for predicting the risk of ALN metastasis is 17.5 and is very easy for clinicians to use. In terms of assessing ALN metastasis, the scoring system showed good performance in the primary (AUC=0.799) and validation cohorts (AUC=0.713), which was similar to the result from Yang et al. [35]. Contrary to previously developed models that might be time-consuming and hard to apply, this risk stratification scoring system provides an easy tool for surgeons to assess breast cancer patients' risk for ALN metastasis prior to surgery [7, 10, 36, 37].

In this study, eight candidates, including AJCC stage, T stage, ER status, HER-2 status, maximum tumor diameter,  $K_{ep}$ ,  $V_e$ , and TTP, were identified as risk factors for ALN metastasis from a stepwise logistic regression model. Our results showed that the selected variables in the scoring system were in line with those of the results reported in previous studies. For instance, Chen et al. found that HER-2 and tumor size were related to breast cancer ALN metastasis [38]. Yang et al. reported that ER and T stage were significantly associated with ALN status [35]. Ya et al. showed the ability of dynamic contrast-enhanced MRI parameters of  $K_{ep}$  and TTP to predict ALN metastasis in breast cancer patients [39]. Among the risk factors in this study, clinicopathologic risk factors for AJCC stage, T stage, ER, and HER-2 were more important than the MRI quantitative parameters of maximum tumor diameter,  $K_{ep}$ ,  $V_e$ , and TTP based on their  $\beta$ -coefficient results in the logistic regression model. These results were consistent with previous results, in which clinicopathological risk factors were better predictors than imaging biomarkers [18, 40]. In addition,  $K_{ep}$  plays a more important role in the PSS than the parameters of  $V_e$  and TTP. The possible



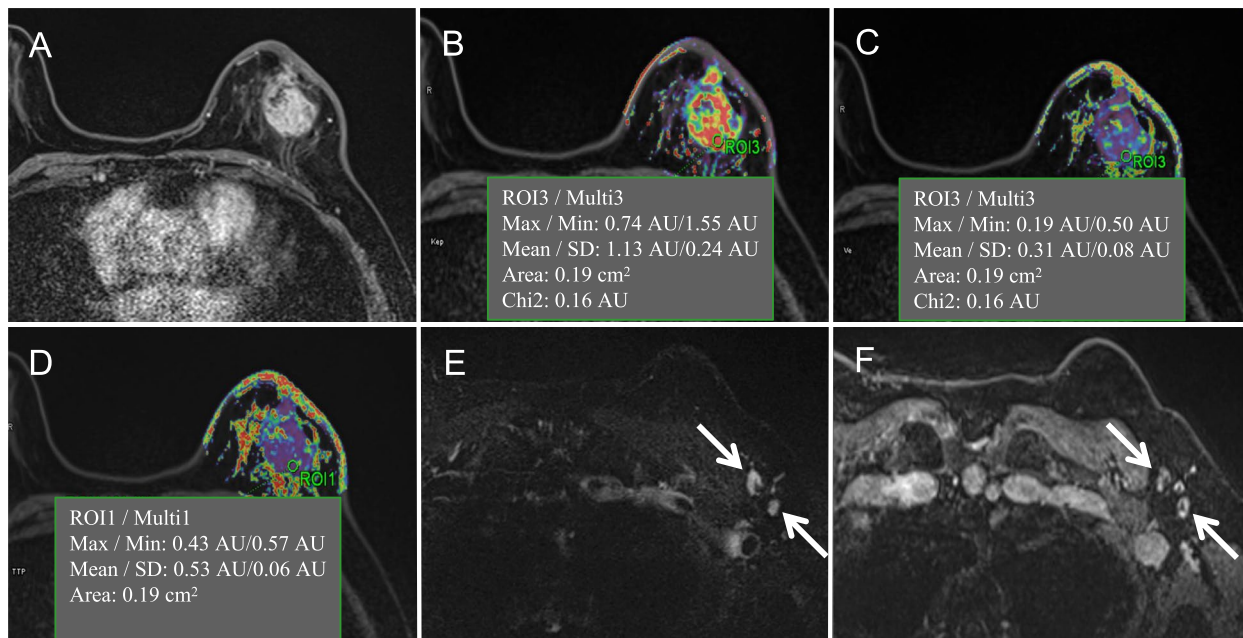


**Fig. 4** One example of the point-based scoring system for predicting breast cancer patients with axillary lymph node metastasis. **A–F** are MRI images of a female left breast cancer patient with invasive ductal carcinoma who was negative for human epidermal growth factor receptor-2, positive for estrogen receptor, AJCC stage II and T2 stage. An axial contrast-enhanced T<sub>1</sub>WI image (**A**) shows a tumor with a maximum diameter of 3.7 cm located in the upper-outer quadrant. The mean values of K<sub>ep</sub>, V<sub>e</sub>, and TTP from the corresponding pseudocolor images of K<sub>ep</sub> (**B**), V<sub>e</sub> (**C**), and TTP (**D**) were 1.130 min<sup>-1</sup>, 0.310, and 0.530 min, respectively. Breast MRI diagnosed no axillary lymph node metastasis for level I nodes due to the lack of all of the following features from axial T<sub>2</sub>WI with fat suppression imaging (**E**) and contrast-enhanced T<sub>1</sub>WI imaging (**F**): cortical thickening, missing fatty hilum, round shape, or a long-to-short axis ratio of less than 2 (long-to-short axis ratio was 2.2 for this patient). However, the risk of axillary lymph node metastasis assessed by the scoring system was 19.5, with an axillary lymph node metastasis probability of 81.8%. The final postoperative pathology report showed that this tumor had three axillary lymph node metastases at axillary level I (white arrow)

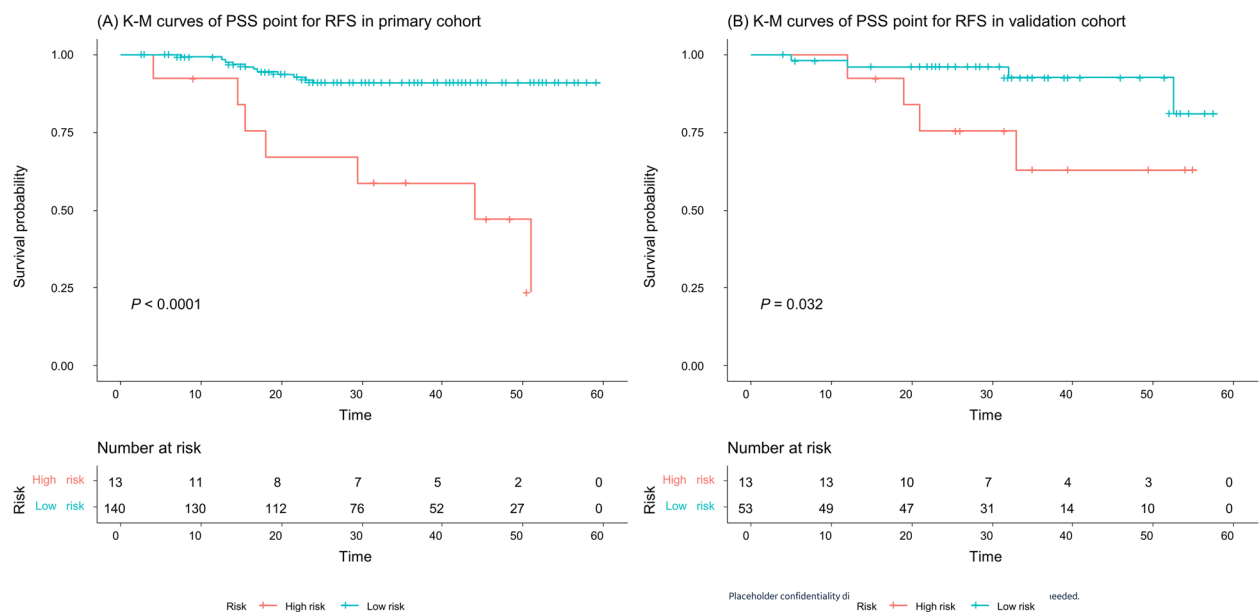


**Fig. 5** Kaplan–Meier recurrence-free survival (RFS) analyses of the low-risk and high-risk groups in the PSS. The high-risk group patients had a significantly worse RFS than the low-risk groups patients in both the primary cohort (**A**) and validation cohort (**B**)

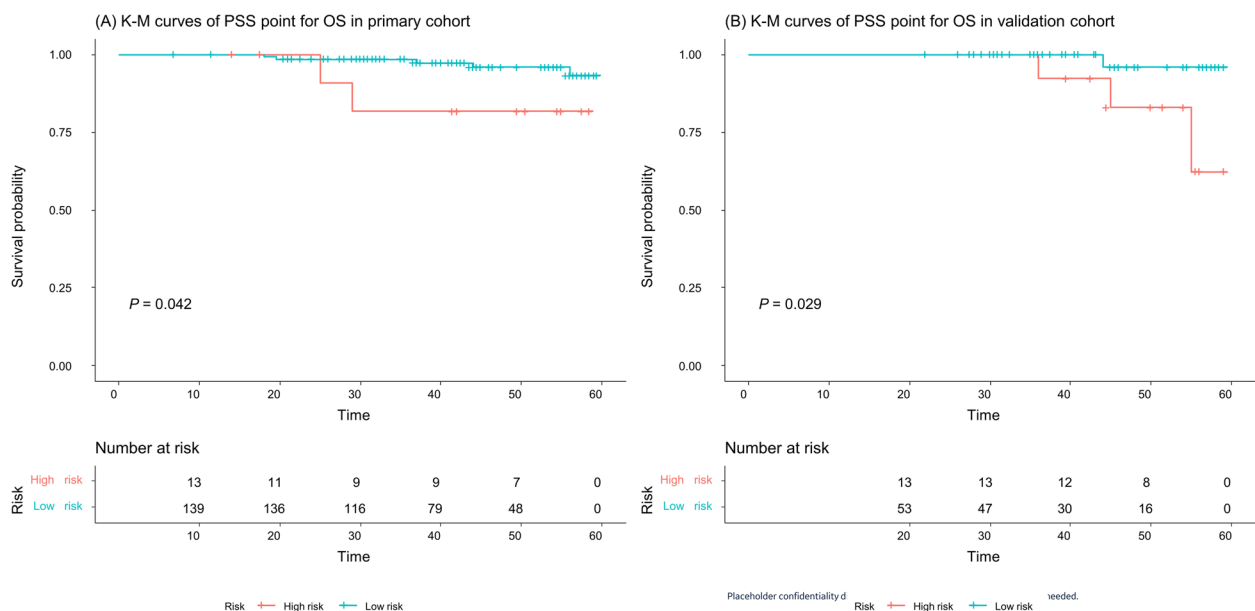


**Fig. 6** Kaplan–Meier overall survival (OS) analyses of the low-risk and high-risk groups in the PSS. The high-risk group patients had a significantly worse OS than the low-risk group patients in both the primary cohort (A) and validation cohort (B)

explanations may be as follows:  $K_{ep}$  may be less sensitive to the absolute value of the contrast agent concentration compared with  $V_e$  and  $TT$ . Another reason could be due to the complexity of the complex pathological characteristics of BC, which were consistent with previous results [28, 41].

The determination of ALN metastasis has important clinical significance for patients' overall recurrence and survival [3, 42]. Generally, patients with ALN metastasis have poor outcomes and a higher risk of local recurrence and distant metastasis than patients without ALN metastasis. Similar results were observed in our study: the patients with ALN metastasis had a higher recurrence rate and overall death rate than the patients without ALN metastasis (recurrence rate: 19.3% vs. 4.5%, and death rate 5.0% vs. 1.8%, respectively). To explore prognostic significance of the PSS, we compared the prognosis of high- and low-risk groups in the PSS. The Kaplan–Meier survival analysis showed that the median RFS and OS of the high-risk group patients were significantly lower than those of the low-risk group patients in both the primary cohort and validation cohort, suggesting that the PSS can be routinely used in predicting the prognosis of BC patients.

This study has several limitations. First, the PSS was developed based on the combination of clinicopathological and MRI features of BC instead of the ALN itself because it is difficult to match the biopsied or dissected ALN on MRI imaging. Second, these retrospective study results were obtained in a single institution with some

inherent limitations and the results should be validated in a multicenter study. Third, some patients were followed up for less than 5 years, which partially affected the strength of prognostic information.

## Conclusion

In conclusion, a simple and reliable point-based scoring system can be used to stratify the ALN metastasis risk of BC. PSS greater than 19.5 was confirmed to be a predictor of short RFS and OS.

## Abbreviations

ALN	Axillary lymph node
BC	Breast cancer
ER	Estrogen receptor
PR	Progesterone receptor
HER-2	Human epidermal growth factor receptor-2
PSS	Point-based scoring system
RFS	Recurrence-free survival
OS	Overall survival

## Supplementary Information

The online version contains supplementary material available at <https://doi.org/10.1186/s40644-023-00564-9>.

**Additional file 1: Table E1.** Shows the MRI acquisition parameters. **Figure E1.** Measurement of MRI quantitative parameters of tumors in a right breast cancer patient with invasive ductal carcinoma.

## Acknowledgements

Not applicable.

**Authors' contributions**

Conceptualization: Zhuozhi Dai, Weixiong Fan. Data curation: Xiaofeng Chen, Zhiqi Yang. Formal analysis: Ruibin Huang, Yue Li. Funding acquisition: Xiaofeng Chen, Zhuozhi Dai. Methodology: Yuting Liao, Guijin Li, Mengzhu Wang. Project administration: Xiangguang Chen, Weixiong Fan. Supervision: Xiangguang Chen, Zhuozhi Dai. Writing—original draft: Xiaofeng Chen, Zhiqi Yang. Writing—review & editing: Zhuozhi Dai, Weixiong Fan. The authors read and approved the final manuscript.

**Funding**

National Natural Science Foundation of China (82101985); Medical Scientific Foundation of Guangdong Province (B2021280).

**Availability of data and materials**

The data cohorts used and/or analyzed in the present study are available from the corresponding authors upon reasonable request.

**Declarations****Ethics approval and consent to participate**

This retrospective study was approved by the institutional review board of Meizhou People's Hospital.

**Consent for publication**

The institutional review board waived the need to obtain informed consent for this retrospective study.

**Competing interests**

One author of the study (YT L) is a consultant for GE Healthcare and was responsible for assisting with data, and another two authors of the study (MZ W) and (GJ L) are consultants for Siemens Healthcare and provided some critical technical support in the manuscript. Those authors have not controlled any data or information that may present a conflict of interest. The other authors are not employees or consultants in the industrial fields and had control of the data and information submitted for publication.

**Author details**

<sup>1</sup>Department of Radiology, Meizhou People's Hospital, Meizhou 514031, China. <sup>2</sup>Guangdong Provincial Key Laboratory of Precision Medicine and Clinical Translational Research of Hakka Population, Meizhou 514031, People's Republic of China. <sup>3</sup>Department of Radiology, The First Affiliated Hospital of Shantou University Medical College, Shantou 515000, People's Republic of China. <sup>4</sup>GE Healthcare, Guangzhou 510623, China. <sup>5</sup>MR Application, Siemens Healthineers, Shanghai 201318, China. <sup>6</sup>MR Scientific Marketing, Siemens Healthineers, Guangzhou 510620, China. <sup>7</sup>Department of Radiology, Shantou Central Hospital, Shantou, Guangdong 515041, People's Republic of China. <sup>8</sup>Department of Radiology, Sun Yat-Sen Memorial Hospital, Sun Yat-Sen University, Guangzhou 510120, Guangdong, China.

Received: 20 October 2022 Accepted: 1 May 2023

Published online: 01 June 2023

**References**

- Poortmans PM, Weltens C, Fortpied C, Kirkove C, Peignaux-Casasnovas K, Budach V, van der Leij F, Vonk E, Weidner N, Rivera S, et al. Internal mammary and medial supraclavicular lymph node chain irradiation in stage I-III breast cancer (EORTC 22922/10925): 15-year results of a randomised, phase 3 trial. *Lancet Oncol*. 2020;21(12):1602–10.
- Zheng X, Yao Z, Huang Y, Yu Y, Wang Y, Liu Y, Mao R, Li F, Xiao Y, Wang Y, et al. Deep learning radiomics can predict axillary lymph node status in early-stage breast cancer. *Nat Commun*. 2020;11(1):1236.
- Chang JM, Leung JWT, Moy L, Ha SM, Moon WK. Axillary nodal evaluation in breast cancer: state of the art. *Radiology*. 2020;295(3):500–15.
- Esposito E, Di Micco R, Gentilini OD. Sentinel node biopsy in early breast cancer. A review on recent and ongoing randomized trials. *Breast*. 2017;36:14–9.
- Magnoni F, Galimberti V, Corso G, Intra M, Sacchini V, Veronesi P. Axillary surgery in breast cancer: An updated historical perspective. *Semin Oncol*. 2020;47(6):341–52.
- Noguchi M, Inokuchi M, Morioka E, Ohno Y, Kurita T. Axillary surgery for breast cancer: past, present, and future. *Breast Cancer* (Tokyo, Japan). 2021;28(1):9–15.
- Zhao M, Wu Q, Guo L, Zhou L, Fu K. Magnetic resonance imaging features for predicting axillary lymph node metastasis in patients with breast cancer. *Eur J Radiol*. 2020;129:109093.
- Zhang J, Li X, Huang R, Feng WL, Kong YN, Xu F, Zhao L, Song QK, Li J, Zhang BN, et al. A nomogram to predict the probability of axillary lymph node metastasis in female patients with breast cancer in China: A nationwide, multicenter, 10-year epidemiological study. *Oncotarget*. 2017;8(21):35311–25.
- Zhang YN, Wang CJ, Xu Y, Zhu QL, Zhou YD, Zhang J, Mao F, Jiang YX, Sun Q. Sensitivity, specificity and accuracy of ultrasound in diagnosis of breast cancer metastasis to the axillary lymph nodes in chinese patients. *Ultrasound Med Biol*. 2015;41(7):1835–41.
- Han L, Zhu Y, Liu Z, Yu T, He C, Jiang W, Kan Y, Dong D, Tian J, Luo Y. Radiomic nomogram for prediction of axillary lymph node metastasis in breast cancer. *Eur Radiol*. 2019;29(7):3820–9.
- An YS, Lee DH, Yoon JK, Lee SJ, Kim TH, Kang DK, Kim KS, Jung YS, Yim H. Diagnostic performance of 18F-FDG PET/CT, ultrasonography and MRI. Detection of axillary lymph node metastasis in breast cancer patients. *Nuklearmedizin*. 2014;53(3):89–94.
- Marino MA, Avendano D, Zapata P, Riedl CC, Pinker K. Lymph node imaging in patients with primary breast cancer: concurrent diagnostic tools. *Oncologist*. 2020;25(2):e231–42.
- Loiselle C, Eby PR, Kim JN, Calhoun KE, Allison KH, Gadi VK, Peacock S, Storer BE, Mankoff DA, Partridge SC, et al. Preoperative MRI improves prediction of extensive occult axillary lymph node metastases in breast cancer patients with a positive sentinel lymph node biopsy. *Acad Radiol*. 2014;21(1):92–8.
- Loiselle CR, Eby PR, DeMartini WB, Peacock S, Bittner N, Lehman CD, Kim JN. Dynamic contrast-enhanced MRI kinetics of invasive breast cancer: a potential prognostic marker for radiation therapy. *Int J Radiat Oncol Biol Phys*. 2010;76(5):1314–9.
- Tuncbilek N, Karakas HM, Okten OO. Dynamic magnetic resonance imaging in determining histopathological prognostic factors of invasive breast cancers. *Eur J Radiol*. 2005;53(2):199–205.
- Ni-Jia-Ti MY, Ai-Hai-Ti DL, Huo-Jia AS, Wu-Mai-Er PL, A-bu-li-zi AB, Shi Y, Rou-zi NE, Su WJ, Dai GZ, Da-mo-la MH. Development of a risk-stratification scoring system for predicting lymphovascular invasion in breast cancer. *BMC Cancer*. 2020;20(1):94.
- Lee MW, Kim GH, Kim KB, Kim YH, Park DY, Choi CI, Kim DH, Jeon TY. Digital image analysis-based scoring system for endoscopic ultrasonography is useful in predicting gastrointestinal stromal tumors. *Gastric Cancer*. 2019;22(5):980–7.
- Chen X, Chen X, Yang J, Li Y, Fan W, Yang Z. Combining Dynamic Contrast-Enhanced Magnetic Resonance Imaging and Apparent Diffusion Coefficient Maps for a Radiomics Nomogram to Predict Pathological Complete Response to Neoadjuvant Chemotherapy in Breast Cancer Patients. *J Comput Assist Tomogr*. 2020;44(2):275–83.
- Chen X, Yang Z, Yang J, Liao Y, Pang P, Fan W, Chen X. Radiomics analysis of contrast-enhanced CT predicts lymphovascular invasion and disease outcome in gastric cancer: a preliminary study. *Cancer Imag*. 2020;20(1):24.
- Yang Z, Chen X, Zhang T, Cheng F, Liao Y, Chen X, Dai Z, Fan W. Quantitative Multiparametric MRI as an imaging biomarker for the prediction of breast cancer receptor status and molecular subtypes. *Front Oncol*. 2021;11(3692):628824.
- Kalli S, Semine A, Cohen S, Naber SP, Makim SS, Bahl M. American Joint Committee on cancer's staging system for breast cancer, eighth edition: what the radiologist needs to know. *Radiographics*. 2018;38(7):1921–33.
- Hamy AS, Lam GT, Laas E, Darrigues L, Balezeau T, Guerin J, Livartowski A, Sadacca B, Pierga JY, Vincent-Salomon A, et al. Lymphovascular invasion after neoadjuvant chemotherapy is strongly associated with poor prognosis in breast carcinoma. *Breast Cancer Res Treat*. 2018;169(2):295–304.
- Health Commission Of The People's Republic Of China N. National guidelines for diagnosis and treatment of breast cancer 2022 in China

- (English version). *Chin J Cancer Res*=Chung kuo yen cheng yen chiu. 2022;34(3):151–75.
24. Liang X, Chen X, Yang Z, Liao Y, Wang M, Li Y, Fan W, Dai Z, Zhang Y. Early prediction of pathological complete response to neoadjuvant chemotherapy combining DCE-MRI and apparent diffusion coefficient values in breast cancer. *BMC Cancer*. 2022;22(1):1250.
  25. Sullivan LM, Massaro JM, D'Agostino RB Sr. Presentation of multivariate data for clinical use: The Framingham Study risk score functions. *Stat Med*. 2004;23(10):1631–60.
  26. Yang Z, Chen X, Huang R, Li S, Lin D, Yang Z, Sun H, Liu G, Qiu J, Tang Y, et al. Atypical presentations of coronavirus disease 2019 (COVID-19) from onset to readmission. *BMC Infect Dis*. 2021;21(1):127.
  27. Zhong M, Yang Z, Chen X, Huang R, Wang M, Fan W, Dai Z, Chen X. Readout-segmented echo-planar diffusion-weighted MR imaging improves the differentiation of breast cancer receptor statuses compared with conventional diffusion-weighted imaging. *J Magnet Reson Imaging*. 2022;56(3):691–9.
  28. Lai T, Chen X, Yang Z, Huang R, Liao Y, Chen X, Dai Z. Quantitative parameters of dynamic contrast-enhanced magnetic resonance imaging to predict lymphovascular invasion and survival outcome in breast cancer. *Cancer Imaging*. 2022;22(1):61.
  29. Wu J, Zhang H, Li L, Hu M, Chen L, Xu B, Song Q. A nomogram for predicting overall survival in patients with low-grade endometrial stromal sarcoma: A population-based analysis. *Cancer Commun (London, England)*. 2020;40(7):301–12.
  30. Turner BM, Gimenez-Sanders MA, Soukiazian A, Breaux AC, Skinner K, Shayne M, Soukiazian N, Ling M, Hicks DG. Risk stratification of ER-positive breast cancer patients: A multi-institutional validation and outcome study of the Rochester Modified Magee algorithm (RoMMA) and prediction of an Oncotype DX<sup>®</sup> recurrence score <26. *Cancer Med*. 2019;8(9):4176–88.
  31. Lai J, Wang H, Peng J, Chen P, Pan Z. Establishment and external validation of a prognostic model for predicting disease-free survival and risk stratification in breast cancer patients treated with neoadjuvant chemotherapy. *Cancer Manage Res*. 2018;10:2347–56.
  32. Li JL, Lin XY, Zhuang LJ, He JY, Peng QQ, Dong YP, Wu JX. Establishment of a risk scoring system for predicting locoregional recurrence in T1 to T2 node-negative breast cancer patients treated with mastectomy: Implications for postoperative radiotherapy. *Medicine (Baltimore)*. 2017;96(26):e7343.
  33. Giuliani M, Rinaldi P, Rella R, D'Angelo A, Carlino G, Infante A, Romani M, Bui E, Belli P, Manfredi R. A new risk stratification score for the management of ultrasound-detected B3 breast lesions. *Breast J*. 2018;24(6):965–70.
  34. Ouldamer L, Chas M, Arbion F, Body G, Cirier J, Ballester M, Bendifallah S, Daraï E. Risk scoring system for predicting axillary response after neoadjuvant chemotherapy in initially node-positive women with breast cancer. *Surg Oncol*. 2018;27(2):158–65.
  35. Yang J, Wang T, Yang L, Wang Y, Li H, Zhou X, Zhao W, Ren J, Li X, Tian J, et al. Preoperative Prediction of Axillary Lymph Node Metastasis in Breast Cancer Using Mammography-Based Radiomics Method. *Sci Rep*. 2019;9(1):4429.
  36. Yu Y, Tan Y, Xie C, Hu Q, Ouyang J, Chen Y, Gu Y, Li A, Lu N, He Z, et al. Development and validation of a preoperative magnetic resonance imaging radiomics-based signature to predict axillary lymph node metastasis and disease-free survival in patients with early-stage breast cancer. *JAMA Netw Open*. 2020;3(12):e2028086.
  37. Arefan D, Chai R, Sun M, Zuley ML, Wu S. Machine learning prediction of axillary lymph node metastasis in breast cancer: 2D versus 3D radiomic features. *Med Phys*. 2020;47(12):6334–42.
  38. Chen W, Wang C, Fu F, Yang B, Chen C, Sun Y. A model to predict the risk of lymph node metastasis in breast cancer based on clinicopathological characteristics. *Cancer Manag Res*. 2020;12:10439–47.
  39. Ya G, Wen F, Xing-Ru L, Zhuan-Zhuan G, Jun-Qiang L. Difference of DCE-MRI parameters at different time points and their predictive value for axillary lymph node metastasis of breast cancer. *Acad Radiol*. 2022;29(Suppl 1):S79–86.
  40. Liu Z, Li Z, Qu J, Zhang R, Zhou X, Li L, et al. Radiomics of multiparametric MRI for pretreatment prediction of pathologic complete response to neoadjuvant chemotherapy in breast cancer: a multicenter study. *Clin Cancer Res*. 2019;25(12):3538–47.
  41. Fedorov A, Fluckiger J, Ayers GD, Li X, Gupta SN, Tempany C, Mulkern R, Yankeelov TE, Fennessy FM. A comparison of two methods for estimating DCE-MRI parameters via individual and cohort based AIFs in prostate cancer: a step towards practical implementation. *Magn Reson Imaging*. 2014;32(4):321–9.
  42. McGale P, Taylor C, Correa C, Cutter D, Duane F, Ewertz M, Gray R, Mannu G, Peto R, Whelan T, et al. Effect of radiotherapy after mastectomy and axillary surgery on 10-year recurrence and 20-year breast cancer mortality: meta-analysis of individual patient data for 8135 women in 22 randomised trials. *Lancet*. 2014;383(9935):2127–35.

## Publisher's Note

Springer Nature remains neutral with regard to jurisdictional claims in published maps and institutional affiliations.

Ready to submit your research? Choose BMC and benefit from:

- fast, convenient online submission
- thorough peer review by experienced researchers in your field
- rapid publication on acceptance
- support for research data, including large and complex data types
- gold Open Access which fosters wider collaboration and increased citations
- maximum visibility for your research: over 100M website views per year

At BMC, research is always in progress.

Learn more [biomedcentral.com/submissions](https://biomedcentral.com/submissions)

